Source process and tectonic implications of the great 1975 North Atlantic earthquake

Christopher S. Lynnes and Larry J. Ruff *Department of Geological Sciences, University of Michigan, Ann Arbor, MI 48109, USA*
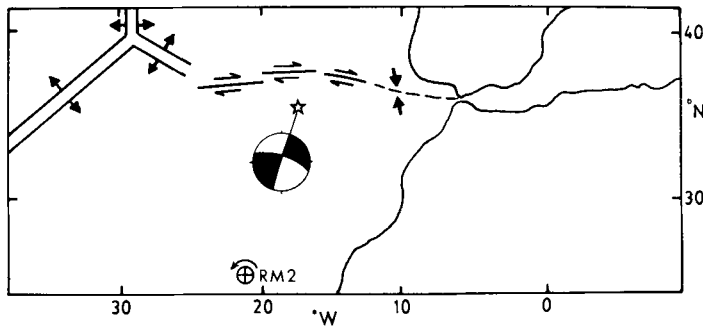
Summary. The Atlantic segment of the Africa–Europe plate boundary has usually been interpreted as a transform boundary on the basis of the bathymetric expression of the Gloria fault and dextral strike-slip first-motion mechanisms aligned along the Azores–Gibraltar line of seismicity. The 1975 May 26 earthquake (M_s=7.9) was assumed to fit into this framework because it occurred in the general area of this line and has a similar first-motion focal mechanism (strike=288°, dip=72°, slip angle=184°). However, several anomalies cast doubt on this picture: the event is abnormally large for an oceanic transform event; a sizeable tsunami was excited; the aftershock area is unusually small for such a large event; and most significantly, the epicentre is 200 km south of the presumed plate boundary. The Rayleigh wave radiation pattern indicates a change in focal mechanism to one with a significant dip-slip component. The short duration of the source time history (20 s, as deconvolved from long-period *P*-waves), the lack of directivity in the Rayleigh waves, and the small one-day aftershock area suggest a fault length less than 80 km. One nodal plane of the earthquake is approximately aligned with the trace of an ancient fracture zone.

We have compared the Pasadena 1-90 record of the 1975 earthquake to that of the 1941 North Atlantic strike-slip earthquake (200 km to the NNW) and confirmed the large size of the 1941 event (M=8.2). The non-colinear relationship of the 1975 and 1941 events suggests that there is no well-defined plate boundary between the Azores and Gibraltar. This interpretation is supported by the intraplate nature of both the 1975 event and the large 1969 thrust event 650 km to the east. This study also implies that the largest oceanic strike-slip earthquakes occur in old lithosphere in a transitional tectonic regime.

1 Introduction

The vast majority of great earthquakes occur as underthrusting events in subduction zones. The 1975 May 26 North Atlantic event (M_s=7.9) is thus unusual in both its location and its focal mechanism. The magnitude is extremely large for an oceanic strike-slip event: the only events of comparable size are the 1981 Macquarie Ridge event (M_w=7.6–7.8; see Ruff, Given & Sanders

1982; Ruff 1983; Dziewonski & Woodhouse 1983), the 1942 Prince Edward West event ($M=7.9$; Gutenberg & Richter 1949, see also Okal & Stewart 1982), the 1941 North Atlantic event ($M=8.2$; Gutenberg & Richter 1949), which occurred about 200 km NNW of the 1975 event and possibly the 1938 Banda Sea event ($M_w=8.5$; see Ben-Menahem 1977). The 1975 earthquake occurred at 35.98°N, 17.56°W at 9:11:51.6 GMT (ISC), placing the event south of the generally accepted plate boundary between Africa and Europe (Fig. 1). The Atlantic segment of this boundary has usually been described as primarily a right-lateral transform with oblique divergence in the west near the Mid-Atlantic Rift and turning to convergence in the east near Portugal (McKenzie 1972; Minster & Jordan 1978; Udias 1980). Indeed, the evidence would seem to support such a configuration. An east–west line of seismicity (albeit a poorly defined one) extends from the Azores triple junction to the Straits of Gibraltar (Fig. 2). First-motion focal mechanisms for the middle part of this line are consistent with right-lateral displacement parallel to the line, while closer to Portugal the focal mechanisms indicate thrust events along fault planes oriented roughly east–west (McKenzie 1972; Udias, Lopez-Arroyo & Mezcua 1976). To the west, Laughton & Whitmarsh (1974) show the Gloria Fault to be a right-lateral transform on the basis of its bathymetry and offset magnetic lineations. Using the orientation of the Gloria Fault and some of the focal mechanisms mentioned above (and including that for the 1975 May 26 event), Minster & Jordan (1978) determined an Euler rotation pole (RM2) of 25.23°N, 21.19°W, about which the African plate

Figure 1. Schematic diagram of the Atlantic segment of the African–European plate boundary, after Udias *et al.* (1976). The location and first-motion mechanism of the 1975 event are shown, together with the rotation pole RM2 of Minster & Jordan (1978).
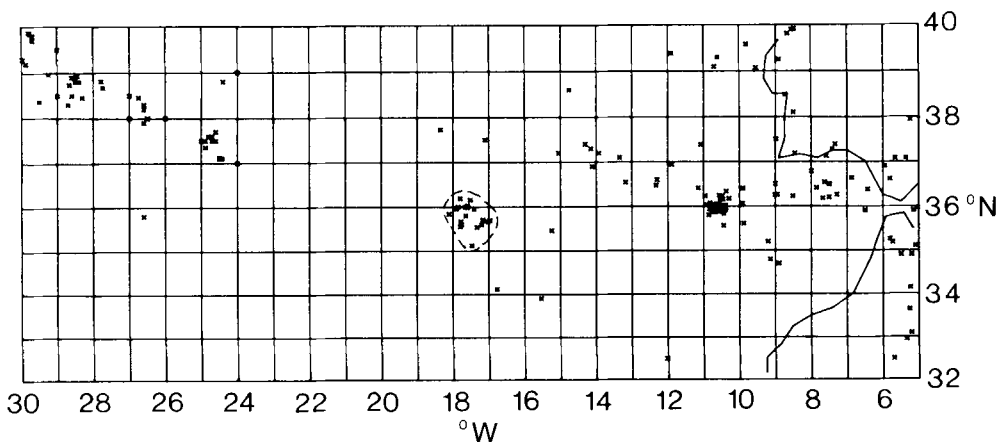

Figure 2. Seismicity between the Azores Islands and Gibraltar during the period 1939–1981 (NEIS). Note the cluster in the centre of the figure, representing the 1975 event and its aftershocks.

rotates counter-clockwise with respect to Europe (Fig. 1). This pole is somewhat NE of McKenzie's (1972) rotation pole (22.7°N, 28.2°W), which was based on spreading rates, fracture zone orientations and earthquake slip vectors. The 1975 May 26 event has a first-motion mechanism that is consistent with the right-lateral transform interpretation (Figs 1 and 3). The mechanism is well constrained and corresponds to almost pure strike-slip if the E–W nodal plane is taken to be the fault plane. Hadley & Kanamori (1975) published a focal mechanism that is somewhat similar (strike, dip, slip angle: $\phi=302°$, $\delta=70°$, $\lambda=196°$) and inferred a unilateral rupture of 150 km to the NW based on G2/G3 spectral ratios. On the basis of these results, the 1975 event fits quite well into the tectonic framework of Minster & Jordan (1978). However, there are several observations that are inconsistent with this interpretation. The aftershock area is at most 100 km long, which is quite small for such a large strike-slip earthquake (Fig. 2). Also, an unusually large tsunami for a strike-slip event, reaching 2 m at Ponta Delgado, Azores (Moreira 1979) was generated. Most importantly, however, the epicentre of this event is actually almost 200 km south of the plate boundary as delineated by the seismicity and represented in the literature (e.g. McKenzie 1972; Laughton & Whitmarsh 1974).

Some observations cast doubt on the overall tectonic framework itself. For instance, the Gloria Fault is in fact devoid of any major seismicity (except possibly at its intersection with the Azores Rise). Another example is the large compressional event of 1969 February 28 near Portugal, which occurred near the probable location of the great 1755 Lisbon earthquake. Using surface waves and aftershocks, Fukao (1973) showed that this earthquake occurred on a steep thrust plane (52°NW) and concluded that it represented a new break in the crust rather than a typical underthrusting event. Finally, Hirn *et al.* (1980) used one-week aftershocks to show that the 1980 January 1 strike-slip event in the Azores ($M_s=6.8$) occurred on a NW-trending sinistral fault plane, rather than the NE-trending dextral plane predicted by the rotation pole.

These anomalies led us to re-examine the rupture process and tectonic implications of the 1975 event.
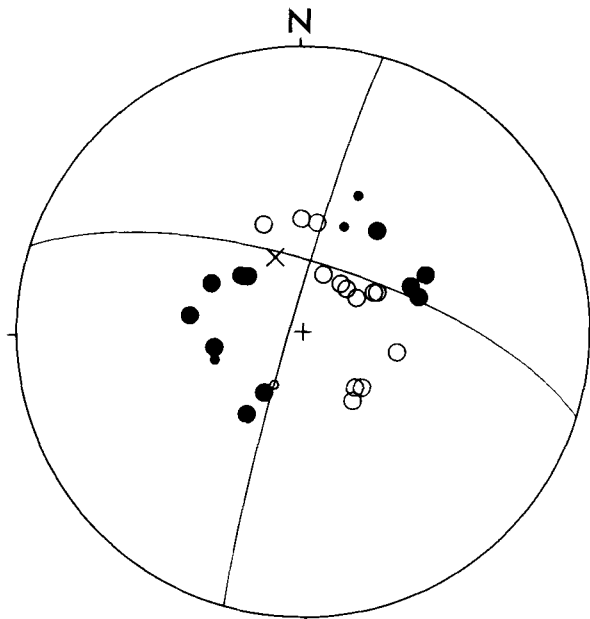
Figure 3. First-motion data and solution for the 1975 North Atlantic event, shown on an equal-area lower hemisphere projection. Open circles are dilatations, closed circles are compressions, ×'s are nodal. Smaller symbols represent less certainty as to polarity. The solution has strike $(\phi)=288°$, dip $(\delta)=72°$, slip angle $(\lambda)=184°$.

17

Data

RAYLEIGH WAVES

Long-period Rayleigh waves (vertical component) and Love waves were equalized to R3 and G3 phases at an epicentral distance of 90° in an effort to constrain the focal mechanism, seismic moment and directivity. The records from Hadley & Kanamori's (1975) study were used, together with several additional WWSSN records. The digitized seismograms were low-pass filtered using a zero-phase filter with a smooth truncation, viz., a half-cosine fitted between 4.3 and 6.0 mHz. This filter eliminates the high-frequency surface waves and yields wave groups with predominant periods of about 210–230 s, serving both to minimize earth structure effects and to isolate the Airy phase for Rayleigh waves.

Mendiguren (1977) showed that focal mechanisms can be uniquely determined from Rayleigh wave amplitudes alone (except for a 180° phase ambiguity) but not from Love wave amplitudes alone for mechanisms with steep fault planes and low slip angles. Thus, the Rayleigh wave radiation pattern is more sensitive to deviations from the first-motion mechanism of the 1975 event than the Love wave radiation pattern. The Rayleigh wave radiation pattern has four lobes for a strike-slip mechanism and two lobes for a pure dip-slip mechanism; the Love wave radiation pattern is four-lobed for all double-couple mechanisms except vertical dip-slip (Kanamori 1970).

The observed Rayleigh wave radiation pattern is four-lobed, but the NW and SE lobes have roughly half the amplitude of the other two lobes (Fig. 4). The average mechanism for the event thus appears to be intermediate between strike-slip and dip-slip. Synthetic seismograms were generated for a point source at a depth of 16 km by the method of Kanamori (1970) and filtered in the same manner as the data for comparison. The best match between the observed and synthetic radiation patterns is for the mechanism $\phi=288°$, $\delta=65°$, $\lambda=205°$ (Fig. 4); but the dip can be varied 5° in either direction if the slip angle is varied comparably in the same direction (i.e. $\delta=70°$, $\lambda=210°$ or $\delta=60°$, $\lambda=200°$). Also, the nodal planes can be rotated about 3° either way in azimuth. The moment obtained by matching observed and synthetic Rayleigh waves is 7×10^{27} dyne cm. There is no resolvable asymmetry in the radiation pattern to indicate directivity, implying either a short fault length or bilateral rupture.

The Rayleigh wave mechanism obtained here has a larger dip-slip component than Hadley & Kanamori's (1975) mechanism and is rotated in azimuth by 14°. More importantly, the Rayleigh wave mechanism has a significantly larger dip-slip component than the first-motion mechanism. To test whether these differences are resolvable, the Rayleigh wave radiation patterns were synthesized for the Hadley–Kanamori mechanism (ignoring directivity) and the first-motion mechanism (Fig. 4). The Hadley–Kanamori pattern is similar to the observed pattern but has larger secondary lobes and is rotated clockwise relative to the data. The radiation pattern for the first-motion mechanism (with no directivity) has lobes of roughly equal amplitude and is clearly incompatible with the observed Rayleigh wave pattern. This difference indicates a resolvable change in focal mechanism during the rupture process from almost pure strike-slip to strike-slip with a significant normal component.

The equalized Rayleigh waves are plotted with the synthetic seismograms, generated for the preferred mechanism and moment, in Fig. 5. The excellent correspondence of the waveforms both confirms the sense of slip (resolving the 180° phase ambiguity) and demonstrates the presence of good long-period signals in the WWSSN seismograms.

LOVE WAVES

We also equalized Love waves to compare the lobe amplitudes to those of the Rayleigh waves in the manner of Abe (1972). The ratio of Love to Rayleigh wave amplitudes generally decreases as
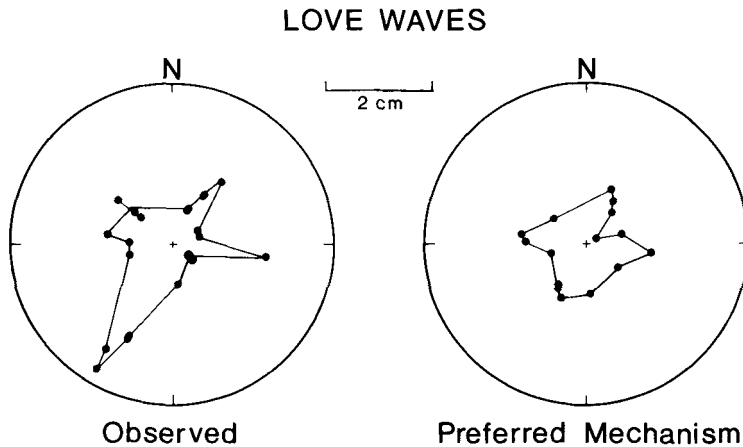
RAYLEIGH WAVES
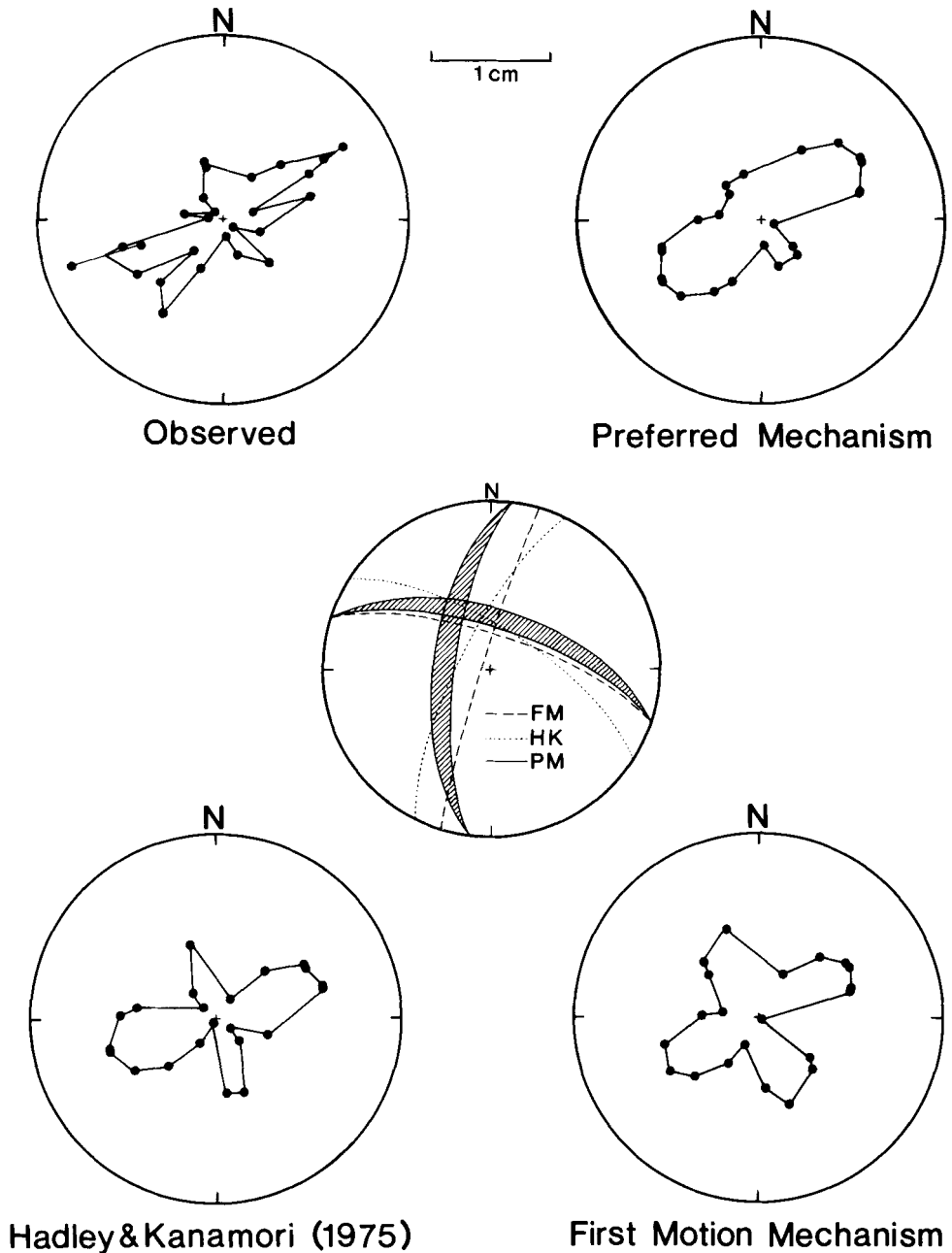
Figure 4. Observed and synthetic Rayleigh wave radiation patterns. The focal mechanisms are plotted together on the lower hemisphere (centre): our preferred Rayleigh wave mechanism (PM: $\phi=288°$, $\delta=65°$, $\lambda=205°$), Hadley & Kanamori's surface wave mechanism (HK: $\phi=302$, $\delta=70°$, $\lambda=196°$), and the first-motion mechanism (FM: $\phi=288°$, $\delta=72°$, $\lambda=184°$); the hachured region shows the range of acceptable solutions for the Rayleigh wave radiation pattern. The synthetic radiation patterns use the same azimuths as the data. Amplitude scale refers to the maximum peak-to-peak amplitude of the filtered Rayleigh wave at a magnification of 1500.
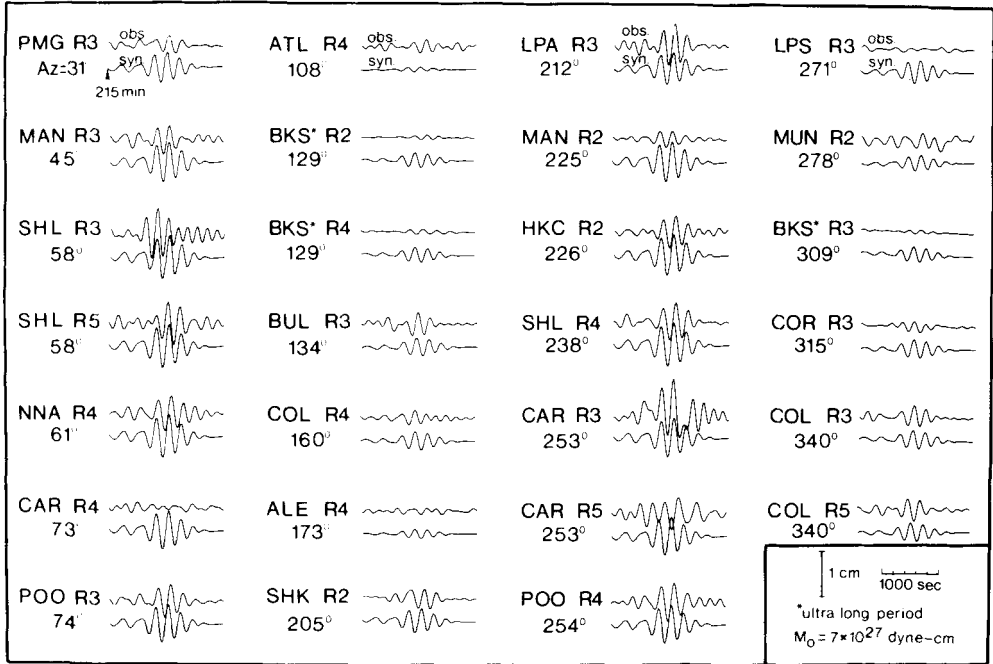
Figure 5. Equalized (top) and synthetic (bottom) Rayleigh waves for all stations used in this study (R3, distance 90°). All recordings are from WWSSN stations except for the ALE (Canadian) and the Berkeley (ultra-long-period) records. The amplitude scale is for a magnification of 1500. The synthetics are generated for a moment of 7×10^{27} dyne cm, using the focal mechanism $\phi = 288°$, $\delta = 65°$, $\lambda = 205°$.

the motion is varied from strike-slip to dip-slip on a given fault plane; but the ratio obtained from the data (about 1.76) is even larger than the ratio for pure strike-slip motion on a fault plane dipping 70° (1.65), while the ratio for the preferred Rayleigh wave mechanism is 1.32. The observed ratio could be matched by increasing the depth to about 30 km. However, both western Love wave lobes are about twice as large as the corresponding eastern lobes (Fig. 6). The

LOVE WAVES



Observed   Preferred Mechanism

Figure 6. Observed and synthetic Love wave radiation patterns, generated using the Rayleigh wave mechanism and moment. Amplitude scale refers to the maximum peak-to-peak amplitude of the filtered Love waves at a magnification of 1500.

existence of this double asymmetry, together with the unusual narrowness of the lobes, suggests that multipathing and focusing-defocusing effects are responsible for the observed asymmetries and may affect the Love/Rayleigh amplitude ratio. To test this hypothesis, ray paths were generated for G2–G4 waves using the ray-tracing method of Lay & Kanamori (1985), which traces surface wavefronts using a ray approximation and the 3-D earth structure of Nakanishi & Anderson (1984). Although the resulting plots show the effect of lateral heterogeneity on amplitudes to be particularly strong, they do not consistently predict the amplitude variation, possibly because Love wave amplitude variations are strongly model-dependent (Schwartz & Lay 1984).

Despite the inconsistencies in the Love wave radiation pattern, there are two important features in the observed pattern that are apparent in the synthetic pattern generated using the mechanism and moment obtained from the Rayleigh waves: (1) the amplitudes agree to within a factor of 2, and (2) the azimuths of the nodal planes are well matched (Fig. 6).

TSUNAMI

The existence of a significant dip-slip component is supported by the tsunami observations. Ward (1980, 1982) and Comer (1984a, b) have shown theoretically that tsunamis can be generated by a strike-slip event, but much less efficiently (about 1/3) than by a dip-slip event.
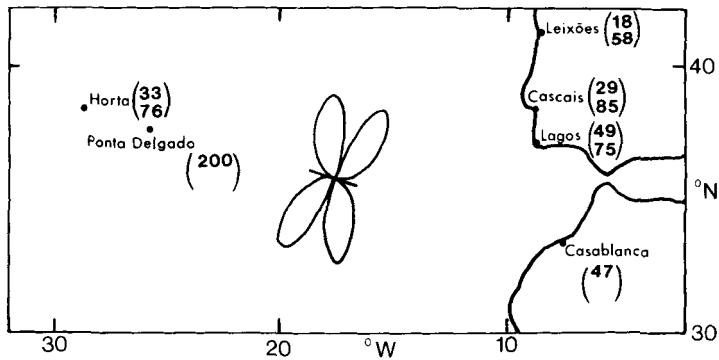

Figure 7. Observed tsunami amplitudes (peak-to-peak) for the 1975 (top) and 1969 (bottom) events, in cm. Data for the 1975 event are from Moreira (1979); data for the 1969 event were measured by the authors from mareograms. A schematic tsunami radiation pattern for a vertical strike-slip fault 222.4 km long, striking 288° (after Ward 1982) is also shown, centred on the epicentre of the 1975 event. Note that Horta and Ponta Delgado are nodal for this radiation pattern.

Also, the tsunami radiation pattern for a point source is similar to that of *P*-waves, and the introduction of a finite fault results in a 'beaming' effect perpendicular to the fault (Ward 1980, 1982). The Azores Islands are almost exactly on a nodal plane for the focal mechanism of the 1975 event (Fig. 7); hence the tsunami should be quite small, particularly if the E–W nodal plane represents a long strike-slip fault plane. Yet a tsunami wave height of 2 m was observed in Ponta Delgado, and other stations report tsunamis that are about 1/3 to 1/2 as large as those generated by the 1969 event, which was a pure thrust (Fig. 7). This suggests: (1) the average mechanism has a larger dip-slip component than the first-motion mechanism, as implied by the Rayleigh waves and (2) either the N–S plane is the fault plane, or the fault length must be small to minimize the beaming effect.

P-WAVES

To characterize the rupture process further, we deconvolved the source–time history of the 1975 event from the long-period P-waves using the time-domain method of Ruff & Kanamori (1983) (Fig. 8). Deconvolutions of several stations for point sources at different depths suggest that the body waves constrain the centroid of the moment release to be shallower than 25 km. A point source representation at 16 km depth and our preferred Rayleigh wave mechanism were used for the final deconvolutions. Unfortunately, the North and South American stations are almost nodal for this mechanism and give less satisfactory results than the Asian and African stations. In all cases, however, the source–time functions are dominated by the initial pulse, lasting 16–22 s. The source–time functions were inverted using the inverse Radon transform method of Ruff (1984) to test the remainder of the source–time functions for directionally coherent moment release. The source–time functions were slant-stacked for all possible rupture
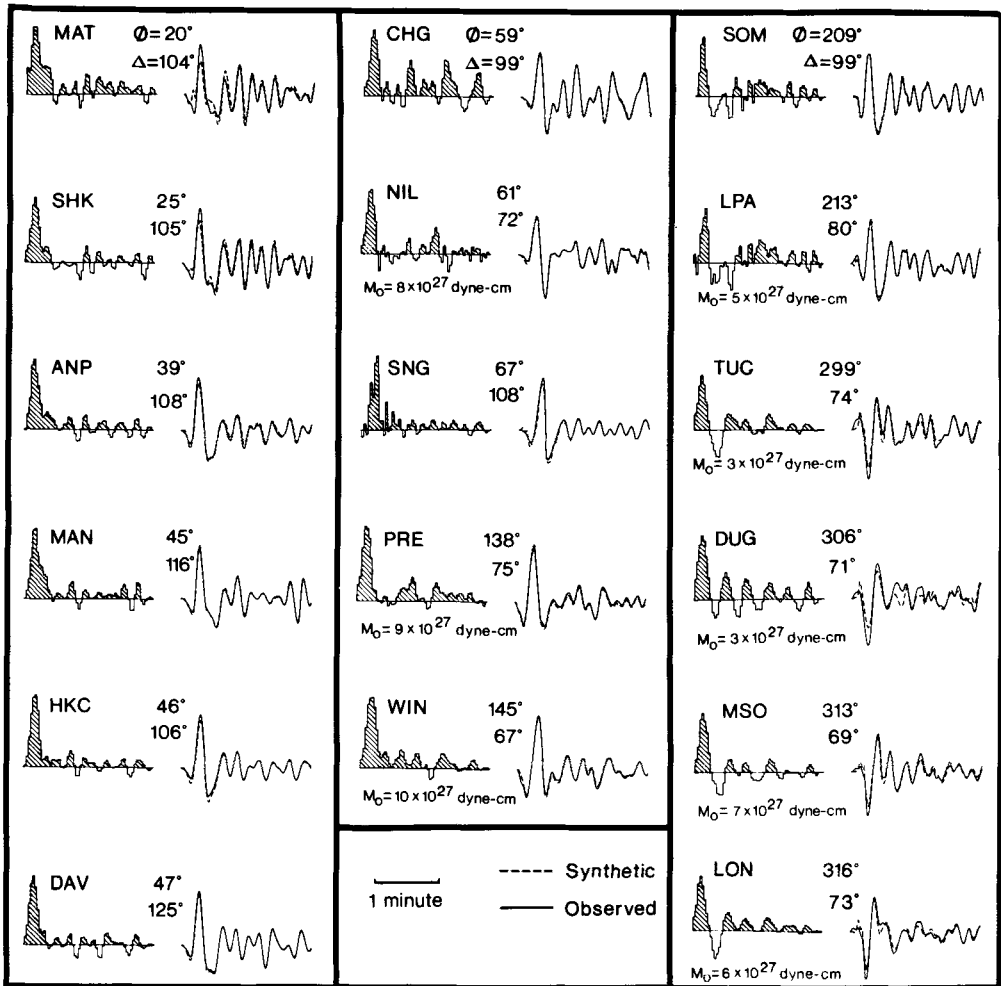

Figure 8. Source–time functions (effective moment rate) of the 1975 North Atlantic earthquake, deconvolved from WWSSN long-period P-waves, with the observed and synthetic seismograms. Azimuth (ϕ) and epicentral distance (Δ) are shown for all stations. The seismic moment is shown only for the undiffracted stations. The average P-wave moment is in good agreement with the surface-wave moment.

Table 1. Station information for surface-wave study.

Station	Azimuth (°)	Distance (°)	Phases used
ALE	353	49	R4, G4
ANP	39	108	G3
ATL	288	54	R4
BKS-ulp	309	79	R2–R4, G2–G5
BKS	309	79	G5
BUL	134	71	R3
CAR	253	51	R3–R5
COL	340	72	R3–R5
COR	315	75	R3
HKC	46	106	R2, G2
LPA	213	80	R3, G2–G3
LPS	271	67	R3, G3
MAN	45	116	R2–R3
MUN	98	142	R2, G1–G2
NNA	241	74	R4, G4
PMG	32	150	R3, G2
POO	74	81	R3–R4, G3–G4
SHK	25	105	R2, G2–G5
SHL	58	90	R3–R5

directions, but no significant coherent moment release after 22 s could be discerned for any rupture direction. Since the surface wave moment and the average body wave moment are in agreement, we conclude that the significant moment release is limited to the initial 16–22 s pulse. Assuming reasonable rupture velocities, the short duration of the 1975 event again implies a short fault length, between 50 and 100 km.
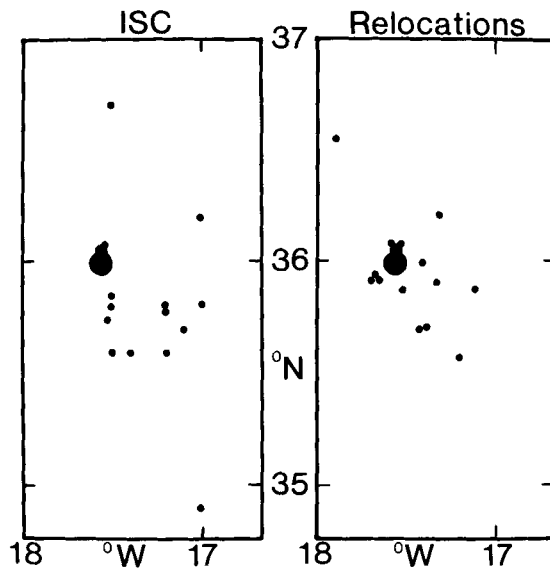
Figure 9. One-day aftershocks using ISC locations and master event relocations. The largest dot is the main shock epicentre, and the intermediate-sized dot represents the only aftershock with a magnitude greater than 5.

AFTERSHOCK AREA

The aftershocks are unusually small in size and number for an event of such magnitude. There is only one of magnitude greater than 5, and only 15 within the first day. The areal extent of the one-day aftershock area is also small, again implying a short fault length. Although the ISC locations are somewhat scattered, the master-event relocations fall quite close to the main shock: none relocate further than 71 km away and all but two fall within about 40 km (Fig. 9). The relocations also show a distinct NW–SE trend. Both the ISC locations and master-event relocations are almost completely confined to the SE of the main shock epicentre, suggesting that the earthquake ruptured to the SE.

We can now estimate the fault dimension and calculate a stress drop. Taking the shear modulus to be 400 kbar, the fault length to be 80 km and the fault width to be 20 km, we obtain a stress drop of 140 bar and a very large displacement of 11 m. This large stress drop is more characteristic of intraplate than interplate large events (Kanamori & Anderson 1975). It should also be noted that the short rupture duration and fault length present a sharp contrast to other large strike-slip earthquakes. The 1976 Guatemala earthquake, for example, has a rupture duration of at least 2 min and a rupture length of 250 km (Kanamori & Stewart 1978), and the 1906 San Francisco and 1857 Fort Tejon events ruptured lengths of 360–400 and 420–470 km respectively (Sieh 1978). Interestingly, the 1981 Macquarie ridge event is intermediate between these and the 1975 event: the rupture duration is about 1 min and the rupture length is less than 150 km (Ruff 1983).

1941 EVENT

The 1941 November 25 earthquake was reported to have a magnitude of 8.2 by Gutenberg & Richter (1949). We have located the epicentre at 37.6°N, 19.1°W using a master-event relocation relative to the 1975 event. The first-motion focal mechanism of this event has been reported as strike-slip by Udias *et al.* (1976) and Di Filippo (1949), with dextral slip on the E–W nodal plane. In order to estimate the size of this event, we compare the Pasadena 1–90 Benioff records for the
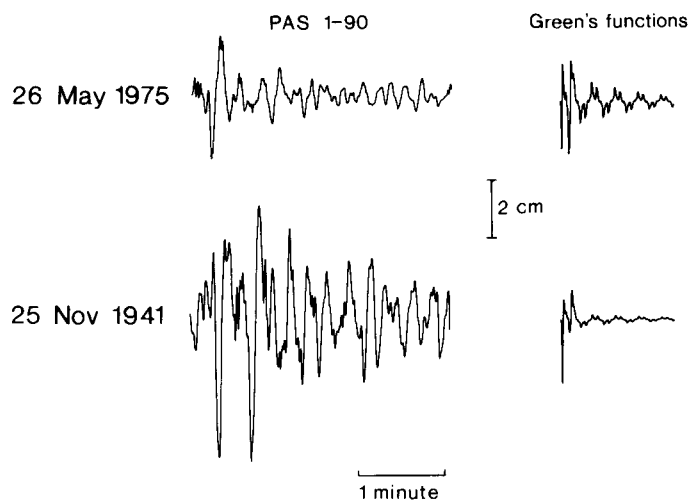
Figure 10. *P*-wave seismograms from the Pasadena 1-90 Benioff instrument for the 1975 May 26 and the 1941 November 25 North Atlantic events. The corresponding *P*-wave Green's functions are generated for PAS using a finite source distributed between 0 and 16 km in depth, moment of 1×10^{27} dyne cm and our preferred mechanism and the Udias *et al.* (1976) mechanism for the 1975 and 1941 events, respectively. Amplitude scale gives the actual trace amplitudes for the 1-90 records.

1975 and 1941 events, together with the Green's functions for a finite source distributed from 0 to 16 km (Fig. 10). The focal mechanism of Udias *et al.* (1976) ($\phi=264°$, $\delta=88°$, $\lambda=186°$) is used for the 1941 event and our Rayleigh wave mechanism is used for the 1975 event. Note that the peak-to-peak amplitudes of the two Green's functions are approximately the same, but the 1941 trace amplitude is about twice as large as the 1975 trace amplitude. Given both the amplitude and the presence of the two pulses in the 1941 record, it is apparent that the 1941 event is at least as large as the 1975 event and may be larger by as much as a factor of 4, thus making it possibly the largest strike-slip event ever recorded.

Regional setting and interpretation

The bathymetry of the seafloor in the area of the 1975 event is shown in Fig. 11, with the epicentres, focal mechanisms, and horizontal projections of the pressure axes of the 1975 event, the 1941 event, and the 1969 thrust event (Fukao 1973) superimposed. The 1975 event apparently occurred on a submarine ridge that has been identified as an ancient fracture zone on the basis of topography and offset magnetic lineations (Laughton & Whitmarsh 1974; Rona 1980). Since the orientation of the fracture zone matches that of the NW–SE nodal plane of our focal mechanism and the trend of the one-day aftershocks, we infer this to be the fault plane. The 1975 event also occurred very close to the Madeira rise, which may have had a significant influence in localizing the earthquake.

The 1941 event occurred on the irregular ridge previously supposed to be the plate boundary. This places it in an *en echelon* or a subparallel relationship to the 1975 event, depending on the direction of rupture, but with no connecting rift. The peculiar relationship between these two great strike-slip earthquakes suggests that there is in fact *no* plate boundary in the conventional sense in this area. Rather, the Africa and Europe plates appear to be in a state of transition, as suggested by Hirn *et al.* (1980); the 1975 event may even represent the birth of a new plate boundary.

The transitional interpretation is further supported by the 1969 event. Fukao (1973) suggested that it represented a crustal break associated with block uplift similar to that which uplifted the Horseshoe Seamounts, as opposed to a typical interplate underthrusting event. The seismic moment calculated by Fukao is 6×10^{27} dyne cm. Thus the majority of the seismic energy released between the Azores and Gibraltar is being released by a few very large events, at least two of which (the 1975 and 1969 events) do not appear to be interplate-style events. It is also interesting that the horizontal projections of the pressure axes for the 1941, 1969 and 1975 earthquakes bear more similarity to each other than do their nodal planes, indicating that the tectonic regime in this area may be better characterized by the prevailing pressure axis orientations than by the slip vector orientations. This is to be expected, however, in the case of intraplate-style earthquakes (e.g. Benioff seismicity within a subducting slab; Isacks, Oliver & Sykes 1968).

Conclusion

The seismic energy release in the vicinity of the presumed Africa–Europe plate boundary is dominated by intraplate-like events. This indicates that this boundary is neither well-defined nor stable, which is further supported by the unusual occurrence of two great strike-slip earthquakes offset 200 km perpendicular to strike. Rather, the boundary seems to be in a state of transition between past and future tectonic regimes. Such a transitional regime should not be unexpected: the African and European continents are in the process of colliding at Gibraltar, and other continent–continent collisions in the past have almost invariably been associated with significant plate tectonic rearrangement.
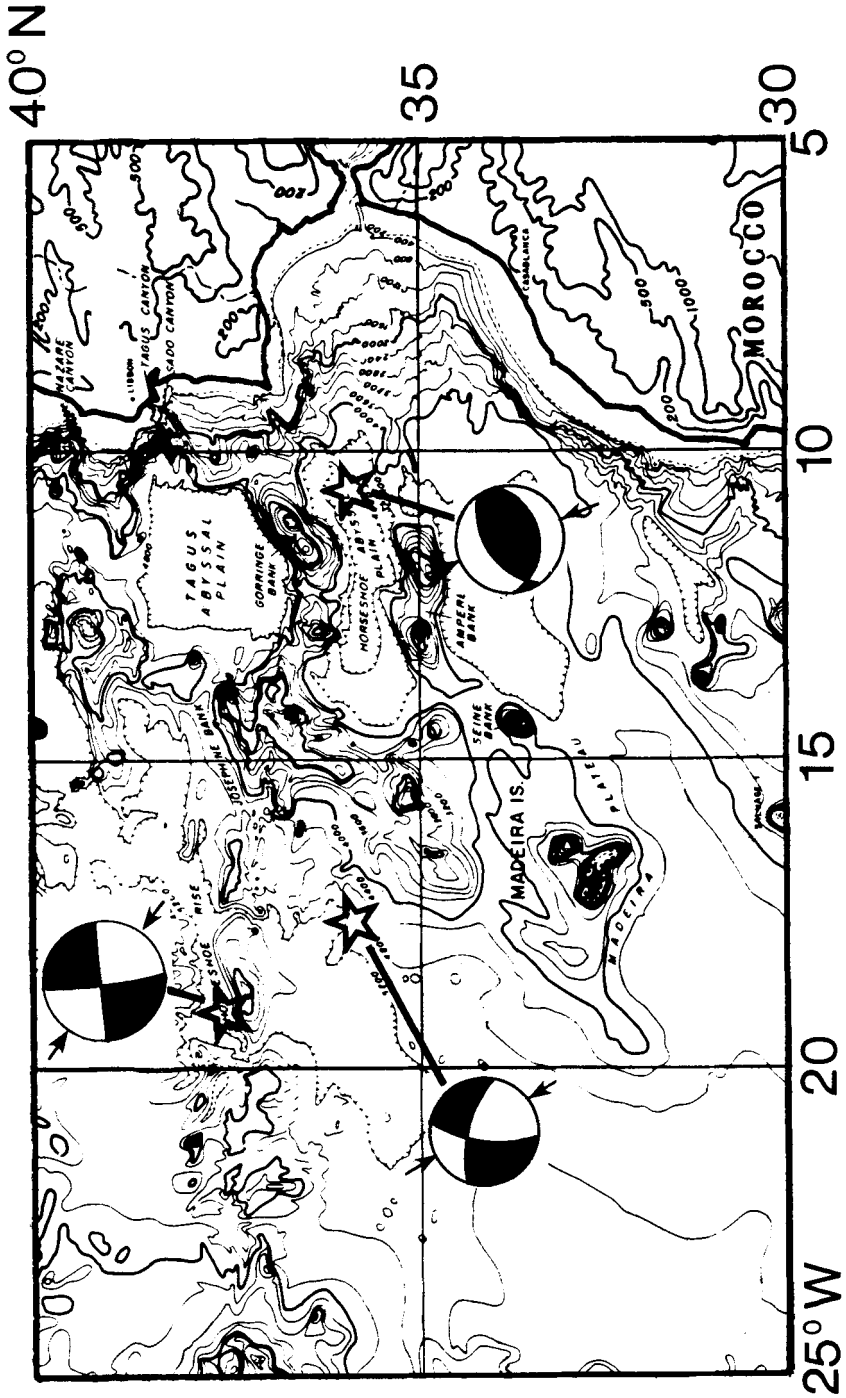
Figure 11. Bathymetry between the Azores and Gibraltar (from Rona 1980). Locations, focal mechanisms and horizontal projections of the pressure axes (arrows) of the 1941 November 25, 1969 February 2 and 1975 May 26 events are shown.

The large size of the 1975 North Atlantic event also raises the question of what conditions are sufficient and/or necessary for the genesis of great strike-slip earthquakes. Three of the largest oceanic strike-slip events (the 1981 Macquarie Ridge and the 1941 and 1975 North Atlantic events) occur where the crust on both sides of the fault is old, i.e. away from oceanic rifts. Wiens & Stein (1983) have suggested that old crust leads to a deeper seismogenic zone in oceanic lithosphere, hence contributing to the seismic moment. Also, the 1981 Macquarie Ridge event, like the North Atlantic events, occurs in a transitional tectonic regime: in this case the rotation pole has been moving south, so that the event occurred in an area which was formerly purely strike-slip but is now obliquely convergent (see Ruff & Cazenave 1985). Although there are still too few great strike-slip earthquakes to define clearly the role of the tectonic regime in determining the size of the event, it would seem that the largest oceanic strike-slip earthquakes occur in transitional tectonic regimes.

Acknowledgments

References

Abe, K., 1972. Mechanisms and tectonic implications of the 1966 and 1970 Peru earthquakes, *Phys. Earth planet. Int.*, **5**, 367–379.

Ben-Menahem, A., 1977. Renormalization of the magnitude scale, *Phys. Earth planet. Int.*, **15**, 315–340.

Comer, R. P., 1984a. The tsunami mode of a flat earth and its excitation by earthquake sources, *Geophys. J. R. astr. Soc.*, **77**, 1–27.

Comer, R. P., 1984b. Tsunami generation: a comparison of traditional and normal mode approaches, *Geophys. J. R. astr. Soc.*, **77**, 29–41.

Di Filippo, D., 1949. Il terremoto delle Azzore del 25 Nov. 1941, *Annali Geofis.*, **2**, 400–405.

Dziewonski, A. M. & Woodhouse, J. H., 1983. An experiment in systematic study of global seismicity: centroid-moment tensor solutions for 201 moderate and large earthquakes of 1981, *J. geophys. Res.*, **88**, 3247–3271.

Fukao, Y., 1973. Thrust faulting at a lithospheric plate boundary, the Portugal earthquake of 1969, *Earth planet. Sci. Lett.*, **18**, 205–216.

Gutenberg, B. & Richter, C. F., 1949. *Seismicity of the Earth*, Princeton University Press.

Hadley, D. M. & Kanamori, H., 1975. Seismotectonics of the eastern Azores-Gibraltar ridge (abstract), *Eos*, **56**, 1028.

Hirn, A., Haessler, H., Hoang Trong, P., Wittlinger, G. & Mendes Victor, L., 1980. Aftershock sequence of the January 1st, 1980 earthquake and present-day tectonics in the Azores, *Geophys. Res. Lett.*, **7**, 501–504.

Isacks, B., Oliver, J. & Sykes, L. R., 1968. Seismology and the new global tectonics, *J. geophys. Res.*, **73**, 5855–5899.

Kanamori, H., 1970. Synthesis of long-period surface waves and its application to earthquake source studies – Kurile Islands earthquake of October 13, 1963, *J. geophys. Res.*, **75**, 5011–5027.

Kanamori, H. & Anderson, D. L., 1975. Theoretical basis of some empirical relations in seismology, *Bull. seism. Soc. Am.*, **65**, 1073–1095.

Kanamori, H. & Stewart, G. S., 1978. Seismological aspects of the Guatemala earthquake of February 4, 1976, *J. geophys. Res.*, **83**, 3427–3434.

Laughton, A. S. & Whitmarsh, R. B., 1974. The Azores–Gibraltar plate boundary, in *Geodynamics of Iceland and the North Atlantic Area*, pp. 63–81, ed. Kristjansson, L., Reidel, Dordrecht.

Lay, T. & Kanamori, H., 1985. Geometric effects of global lateral heterogeneity on long-period surface wave propagation, *J. geophys. Res.*, **90**, 605–621.

McKenzie, D., 1972. Active tectonics of the Mediterranean region, *Geophys. J. R. astr. Soc.*, **30**, 109–185.

Mendiguren, J., 1977. Inversion of surface wave data in source mechanism studies, *J. geophys. Res.*, **82**, 889–894.

Minster, J. B. & Jordan, T. H., 1978. Present-day plate motions, *J. geophys. Res.*, **83**, 5331–5354.

Moreira, V. S., 1979. *Report of activities in Europe during the period 1975–1979*, presented to the IUGG Tsunami Committee, Canberra.

Nakanishi, I. & Anderson, D. L., 1984. Measurements of mantle wave velocities and inversion for lateral heterogeneity and anisotropy – II. Analysis by the single station method, *Geophys. J. R. astr. Soc.*, **78**, 573–617.

Okal, E. A. & Stewart, L. M., 1982. Slow earthquakes along oceanic fracture zones: evidence for asthenospheric flow away from hotspots?, *Earth planet. Sci. Lett.*, **57**, 75–87.

Rona, P. A., 1980. The central north Atlantic ocean basin and continental margins: geology, geophysics, geochemistry, and resources, including the trans-Atlantic geotraverse (TAG), *NOAA atlas 3*.

Ruff, L. J., 1983. Fault asperities inferred from seismic body waves, in *Earthquakes: Observation, Theory and Interpretation*, pp. 251–276, eds Kanamori, H. & Boschi, E., Elsevier-North Holland, New York.

Ruff, L. J., 1984. Tomographic imaging of the earthquake rupture process, *Geophys. Res. Lett.*, **11**, 629–632.

Ruff, L. J. & Cazenave, A., 1985. SEASAT geoid anomalies and the Macquarie Ridge complex, *Phys. Earth planet. Int.*, **38**, 59–69.

Ruff, L. J., Given, J. & Sanders, C., 1982. The tectonics of the Macquarie Ridge, New Zealand: new evidence of strike-slip motion from the earthquake of May 25, 1981, M_w=7.7 (abstract), *Eos*, **63**, 384.

Ruff, L. J. & Kanamori, H., 1983. The rupture process and asperity distribution of three great earthquakes from long-period diffracted *P*-waves, *Phys. Earth planet. Int.*, **31**, 202–230.

Schwartz, S. Y. & Lay, T., 1984. Comparison of surface wave amplitude and phase anomalies for two models of global lateral heterogeneity (abstract), *Eos*, **65**, 1003.

Sieh, K. E., 1978. Slip along the San Andreas fault associated with the great 1857 earthquake, *Bull. seism. Soc. Am.*, **68**, 1421–1448.

Udias, A., 1980. Seismic stresses in the region Azores-Spain-Western Mediterranean, *Suppl. Rock Mech.*, **9**, 75–84.

Udias, A., Lopez-Arroyo, A. & Mezcua, J., 1976. Seismotectonics of the Azores-Alboran region, *Tectonophys.*, **31**, 259–289.

Ward, S. N., 1980. Relationships of tsunami generation and an earthquake source, *J. Phys. Earth*, **28**, 441–474.

Ward, S. N., 1982. On tsunami nucleation II. An instantaneous modulated line source, *Phys. Earth planet. Int.*, **27**, 273–285.

Wiens, D. A. & Stein, S., 1983. Age dependence of intraplate seismicity and implications for lithospheric evolution, *J. geophys. Res.*, **88**, 6455–6468.